SPhT/02-093

Census of Planar Maps: From the One-Matrix Model Solution to a Combinatorial Proof

J. Bouttier[1], P. Di Francesco[2] and E. Guitter[3]

Service de Physique Théorique, CEA/DSM/SPhT

Unité de recherche associée au CNRS

CEA/Saclay

91191 Gif sur Yvette Cedex, France

We consider the problem of enumeration of planar maps and revisit its one-matrix model solution in the light of recent combinatorial techniques involving conjugated trees. We adapt and generalize these techniques so as to give an alternative and purely combinatorial solution to the problem of counting arbitrary planar maps with prescribed vertex degrees.

07/02

[1] bouttier@spht.saclay.cea.fr

[2] philippe@spht.saclay.cea.fr

[3] guitter@spht.saclay.cea.fr

1. Introduction

Enumeration of planar maps has been a classical subject of combinatorics originally motivated by the famous four-color problem. Major advances in this field were obtained in the 60's by W. Tutte in his famous "Census" papers [1-4], giving many explicit enumerations for various classes of planar maps. Fifteen years later, the same problem became popular among physicists in the context of the perturbative expansion of SU(N) gauge field theory [5]. Indeed, at large N, the dominant Feynman diagrams correspond precisely to planar maps. Explicit enumeration formulas extending previous results were derived by matrix integral techniques [6], a tool which proved very powerful for such problems. Even more recently, planar maps were used in physics as tessellations of random surfaces, in the context of both discretized 2D quantum gravity and fluid membranes (see e.g. [7] and [8]).

Planar maps are formally defined as proper embeddings of graphs into the two-dimensional Riemann sphere, considered up to continuous deformations. A map is characterized by a number of *vertices*, *edges* and *faces*. The general question we address here is the enumeration all such maps with prescribed vertex degrees, i.e, for each k, a fixed number n_k of k-valent vertices. Turning to generating functions, we can instead consider the partition function of all maps with a weight g_k per k-valent vertex. It proves also useful to introduce an additional weight t per edge so that a term of given degree in t accounts for a finite number of maps.

The effective counting can be performed in a mechanical way by solving the generic one-matrix model with standard techniques. This approach provides directly the net result, but its powerful nature may seem magical as it hides all the combinatorial aspects of the problem, and some of its calculations must be understood in a purely formal way. Recently, a new purely combinatorial method for studying planar maps was developed, using so-called conjugacy classes of trees, allowing for a new derivation of Tutte's results as well as some generalizations (see [9] for a review). In comparison to our present goal, this approach was restricted to the enumeration of Eulerian planar maps, i.e. maps with only vertices of *even* valences.

In this paper, we give a combinatorial solution of the general problem of enumeration of planar maps with arbitrary valences, generalizing the method of conjugated trees and elucidating the combinatorial structure of the one-matrix model solution. The paper is organized as follows. In Section 2, we introduce the quantities of interest and recall their expression as provided by the one-matrix model (corresponding derivations are detailed in

appendix A). In Section 3, we present our combinatorial proof. We first define appropriate decorated trees whose enumeration makes the connection with the one-matrix model solution. We then establish bijections between classes of such trees and planar maps. Particular cases are discussed in Section 4 and conclusions are gathered in Section 5.

2. Solution via matrix integral

2.1. Definitions

Let us now come to the precise definition of the various generating functions that we wish to compute.

Planar maps may display a large number of internal symmetries making the counting quite subtle. Indeed, in both matrix integral and combinatorial approaches, maps are naturally counted with an inverse symmetry weight. A convenient way to avoid this problem is to consider instead *rooted* maps, with a marked oriented edge which lifts up ambiguities due to symmetries. We will denote by $E(t;\{g_k\}_{k\geq 1})$ the generating function for rooted planar maps.

Beside these "closed diagrams", it will prove convenient to also consider *one-leg diagrams*, namely planar maps with a distinguished univalent vertex (the endpoint of the external leg). For these diagrams, no symmetry problem arises and we denote by $\Gamma_1(t;\{g_k\})$ their generating function with no weight for the distinguished vertex.

Finally, we will also consider the generating function $\Gamma_2(t;\{g_k\})$ for *two-leg diagrams* with two unweighted distinguished (as, say, incoming and outcoming) univalent vertices *adjacent to the same face.*

Examples of maps contributing to E, Γ_1 and Γ_2 are displayed in Fig. 1. Our convention to represent maps in the plane is to choose as the external face that on the right of the marked edge for closed diagrams, and that adjacent to the distinguished vertices for both one- and two-leg diagrams.

When cutting the marked edge in a rooted closed map, we get either two disconnected one-leg diagrams, or a two-leg diagram with legs in the same face, excluding that formed by a single oriented edge. This leads to the first general relation

$$E = \frac{\Gamma_1^2 + \Gamma_2 - t}{t} \tag{2.1}$$

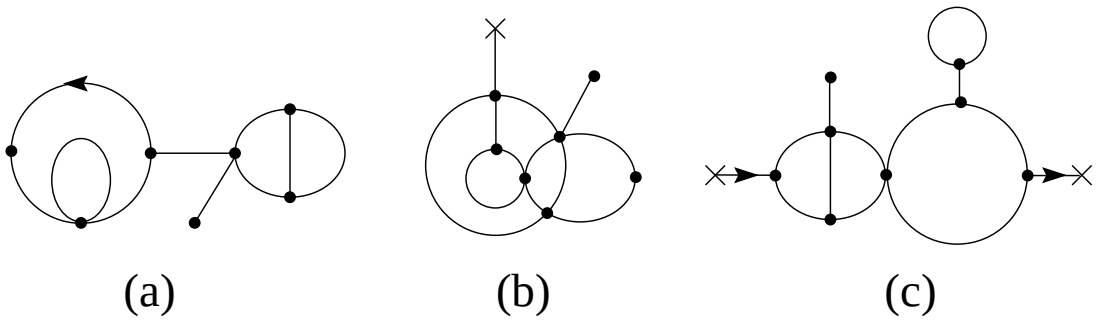

Fig. 1: Typical planar maps contributing respectively to the generating functions E, Γ_1 and Γ_2, namely (a) a rooted planar map with one regular univalent, one bivalent, three trivalent and two tetravalent vertices; (b) a one-leg diagram with one regular univalent, one bivalent, one trivalent, three tetravalent and one pentavalent vertices; (c) a two-leg diagram with one regular univalent, five trivalent and two tetravalent vertices. In the first case, the rooted edge is marked by an arrow. In the two latter, the distinguished univalent vertices attached to the external legs are marked by a cross. In (c), the two legs must lie in the same face and are distinguished as in- and outcoming via an orientation.

2.2. One-matrix model results

Formally, all quantities of interest can be obtained as the large N limit of average values in a $N \times N$ one-matrix model with partition function

$$Z = \int dM \exp N\mathrm{Tr}\left(-\frac{M^2}{2t} + \sum_{k\geq 1}\frac{g_k}{k}M^k\right) \tag{2.2}$$

where dM denotes the standard Haar ($\mathrm{SU}(N)$ invariant) measure over hermitian matrices (see e.g. [7] and [8] for details).

As shown in appendix A, the solution of the problem involves two functions $S(t;\{g_k\})$ and $R(t;\{g_k\})$ characterizing the eigenvalue distribution at large N. Introducing the potential

$$V(x) = \sum_{k\geq 1}\frac{g_k}{k}x^k \tag{2.3}$$

and the formal parametrization

$$Q(z) = z + S + R/z \tag{2.4}$$

in terms of a dummy variable z, the functions S and R are implicitly determined by

$$\begin{aligned} S &= tV'(Q)|_{z^0} \\ R &= t + tV'(Q)|_{z^{-1}} \end{aligned} \tag{2.5}$$

where $V'(Q)|_{z^m}$ denotes the coefficient of z^m in $V'(Q)$ when viewed as a Laurent series in z. The correct determination is fixed by $S(0;\{g_k\}) = R(0;\{g_k\}) = 0$, allowing for an expansion as a power series in t.

The generating functions for maps are then given in terms of S and R through

$$\begin{aligned} \Gamma_1 &= S - V'(Q)|_{z^{-2}} \\ \Gamma_2 &= R - V'(Q)|_{z^{-3}} - \left(V'(Q)|_{z^{-2}}\right)^2 \end{aligned} \tag{2.6}$$

and E follows from Eq. (2.1).

In principle, the above equations solve the enumeration problem. In practice, the generic term of the series can be computed explicitly in simple cases such as cubic maps ($g_k = 0$ when $k \neq 3$), or Eulerian maps ($g_k = 0$ for odd k) as discussed in Section 4 below. As an illustration, we list the first few terms in Eq. (2.5) by expanding the potential (2.3) up to the quartic term

$$\begin{aligned} S &= tg_1 + tg_2 S + tg_3(S^2 + 2R) + tg_4(S^3 + 6RS) + \cdots \\ R &= t + tg_2 R + tg_3(2RS) + tg_4(3S^2 R + 3R^2) + \cdots \end{aligned} \tag{2.7}$$

which can be solved order by order in t with the initial conditions $R = t + O(t^2)$, $S = tg_1 + O(t^2)$.

In the next Section, we will recover precisely the same set of equations through a purely combinatorial approach.

3. Combinatorial Solution

We now come to the core of the paper, namely the combinatorial rederivation of the above equations (2.5) and (2.6). We first show that the functions S and R are indeed generating functions of decorated "blossom trees" generalizing those introduced for the counting of Eulerian maps in Ref. [10]. These trees are to be closed into graphs to recover planar maps. As in Ref. [10], bijections can be established between planar maps and properly defined conjugacy classes of these trees, which we will describe precisely. We will show the equivalence to planar maps both in the case of one-leg and two-leg diagrams, allowing to recover all the results of the matrix model described above.

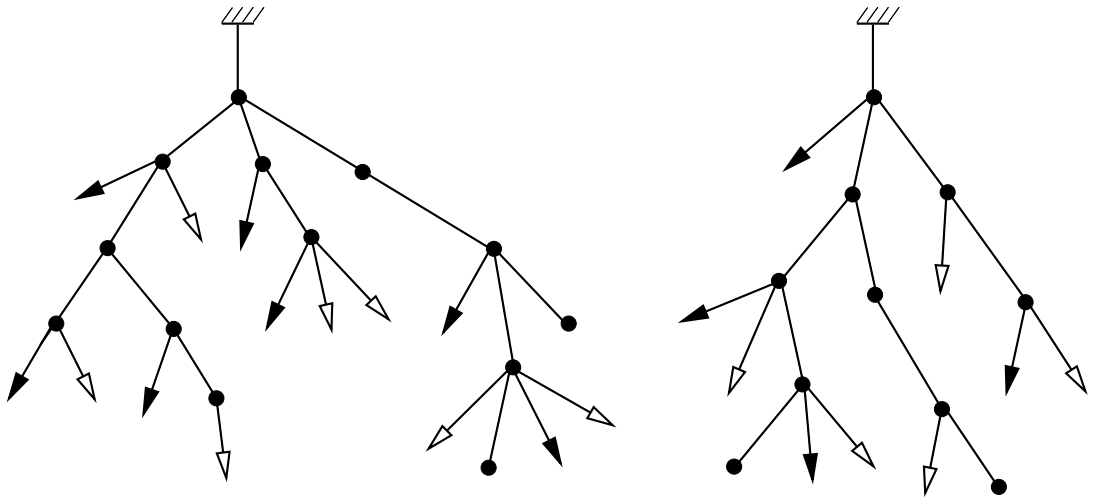

Fig. 2: A typical S-tree (S) and a typical R-tree (R). The leaves are represented with empty arrows, buds correspond to filled black arrows, while regular vertices are solid black dots. The leaves carry a charge $+1$ while the buds carry a charge -1. The S-tree has a total charge 0 (7 leaves and 7 buds), while the R-tree has a total charge 1 (5 leaves and 4 buds). Both have the property that any descendent subtree not reduced to a bud has total charge 0 or 1.

3.1. Rooted blossom trees

Let us now define rooted S- and R- *blossom trees*. These are (finite) rooted planar trees with three species of endpoints that we will refer to as *leaves*, *buds*, and regular univalent vertices. We assign a "charge" $q = +1$ (resp. $q = -1$) to leaves (resp. buds), while regular univalent vertices remain neutral ($q = 0$). These trees are called S- (resp. R-) trees iff: (i) their total charge is 0 (resp. 1) and (ii) any descendent subtree not made of a single bud has total charge 0 or 1.

As an example, the smallest S-tree is made of a single regular univalent vertex attached to the root while the smallest R-tree is made of a single leaf attached to the root. Typical S- and R- trees are represented in Fig. 2.

Obviously, any descendent subtree of an S- or R-tree not reduced to a bud is itself an S- or an R-tree. This recursive property allows to interpret the functions S (resp. R) of Eq. (2.5) as the generating functions for rooted S-trees (resp. R-trees) with a weight g_k per k-valent vertex ($k \geq 1$) and a weight t per edge not leading to a bud. First, we note that the dummy variable z in Eq. (2.4) may be thought of as a fugacity per unit of charge. Viewing the three terms in $Q(z) = z + S + R/z$ as associated respectively to a

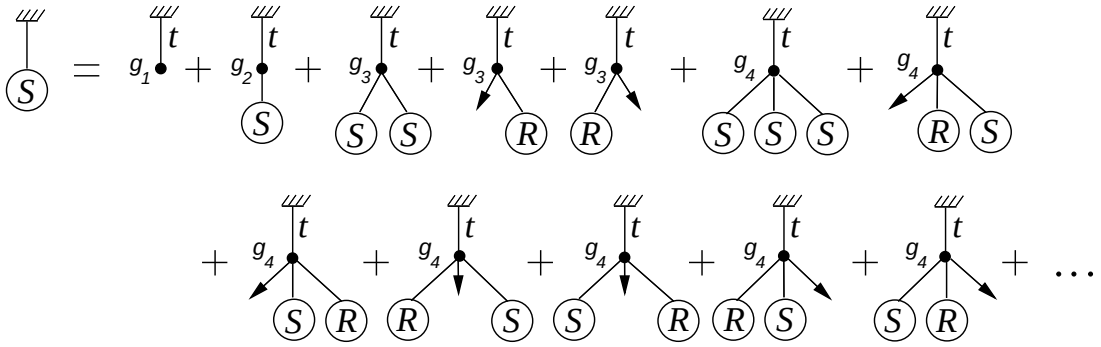

Fig. 3: Illustration of the recursive generation of a rooted S-tree via the enumeration of all possible vertices of total charge 0 attached to the root for terms up to g_4 in the potential V. This parallels the first line of the recursion (2.7) by viewing the labels S and R as generating functions for S- and R-trees.

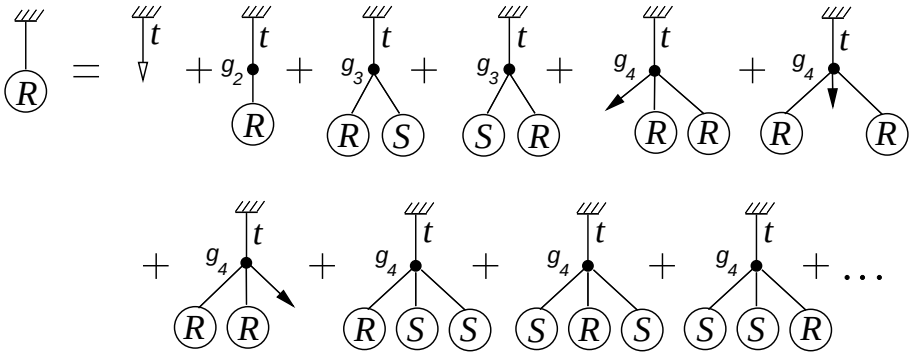

Fig. 4: The same illustration as in Fig. 3 for a rooted R-tree (with now vertices of total charge 1), to be paralleled with the second line of the recursion (2.7) for terms up to g_4 in the potential V.

bud ($q=-1$), an S-tree ($q=0$) and an R-tree ($q=+1$), the power of $1/z$ measures the total charge of any composite object. This allows to interpret $V'(Q)|_{z^{-m}}$ as generating all possible vertices with descendents being buds, S-trees and R-trees, with a total charge $q=m$ and with weight g_k per k-valent vertex (i.e. with $(k-1)$ descendents). Expressions (2.5) for S-trees and R-trees follow by enumeration of all possible configurations around the vertex attached to the root, with a total charge of 0 and 1 respectively. The factor t in front of $V'(Q)$ accounts for the weight of the root edge, while the additional t term in R stands for the germ of the recursion. These recursions are depicted in Figs. 3 and 4, for the first few terms involving 1, 2, 3 and 4-valent vertices.

3.2. Conjugated trees

Starting with the above S- and R-trees, we may now wipe out the root by replacing it by a standard (unmarked) leaf, thus increasing the total charge by one unit. This defines

unrooted S- and R-trees with total charge 1 and 2 respectively. Two rooted S- (resp. R-) trees are said to belong to the same *conjugacy class* iff they lead to the same unrooted tree.

The case of S-trees is simple in that reciprocally, given any unrooted S-tree, we obtain all the corresponding rooted S-trees by picking *any* of its leaves and choosing it as the root. This leads to a n-to-one correspondence between rooted and unrooted S-trees with n leaves (including the former root). The proof goes as follows. Recall first that cutting any edge not leading to a bud in a rooted S-tree cuts out a descendent subtree of charge 0 or 1. Consequently, cutting the same edge in the corresponding unrooted S-tree separates the tree into a piece of charge 0 or 1 and a complementary piece of charge 1 or 0 respectively, as the total charge is 1. This property, valid for any edge not leading to a bud, completely characterizes the unrooted S-trees. Indeed, starting from an unrooted tree with this property, we see that it has total charge 1, and that therefore by replacing an arbitrary leaf by a root, we end up with a rooted tree of total charge 0 whose descendent subtrees not reduced to a bud have charge 0 or 1, the characterization of rooted S-trees. As the choice of leaf taken as a root is arbitrary among the n leaves, this moreover shows that the conjugacy class is made of n rooted S-trees, by finally noting that the unrooted S-trees have no accidental rotational symmetry since the numbers of buds $(n-1)$ and leaves (n) are coprime. This completes the abovementioned n-to-one correspondence. A last remark is in order: cutting any edge not leading to a bud of an unrooted S-tree separates the tree into two rooted trees, one being a rooted S-tree and the other a rooted R-tree. Indeed these trees have respective charges 0 and 1 and any of their descendent subtrees not made of a single bud also have charge 0 or 1 as pieces of the unrooted S-tree.

The case of R-trees is more subtle. Indeed, it is no longer true that picking as a root any leaf of an unrooted R-tree leads to a rooted R-tree. In order to characterize the subset of *admissible* leaves (leading effectively to rooted R-trees), we first define the *core* of an unrooted R-tree by the following procedure: (i) we mark all the inner edges which separate the tree into two pieces of respective charge 0 and 2, (ii) we remove all these edges and (iii) we define the core as the only connected component with total charge 2. This is illustrated in Fig. 5. To show the existence and uniqueness of the core, we consider an arbitrary admissible leaf and the corresponding rooted R-tree. Due to charge constraints, an edge is marked at step (i) iff the descendent subtree originating from it is an S-tree. Such a subtree is then amputated from its own S-subtrees, splitting eventually into connected components all of charge 0. The connected component containing the root is the only one not obtained

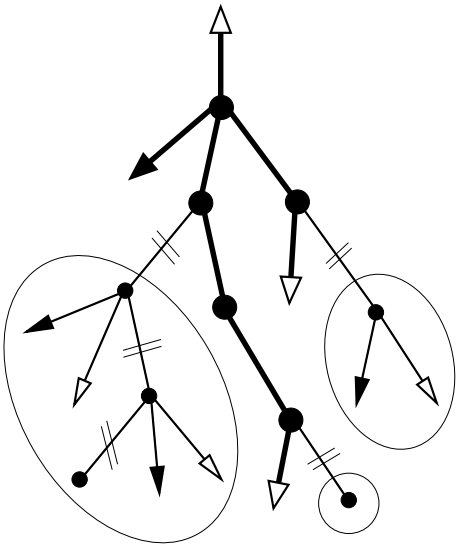

Fig. 5: The core of a typical unrooted R-tree. We have indicated by double-lines the edges "of type 0-2" to be cut in the core construction process. The circled pieces are the maximal S-subtrees (of charge 0) attached to the core (of charge 2), represented in thick lines. In this particular example, the core has three leaves and one bud.

in this way, hence it has charge 2. Note also that all trees attached to the core are rooted S-trees attached by their root. We call them *maximal* S-subtrees. As our procedure was defined independently of the admissible root at hand, it follows that all admissible leaves belong to the core. Conversely, replacing an arbitrary leaf in the core by a root, we get a rooted tree such that any descendent subtree not made of a single bud either is contained in an S-subtree, or originates from an edge in the core not marked at step (i): in both cases its total charge is 0 or 1 as wanted. To conclude, the conjugacy class associated with an unrooted R-tree is made of all trees rooted at leaves of the core. As opposed to the S-case, care must be taken with a possible two-fold rotational symmetry (half turn) which is the only one compatible with the fact that there are two more leaves than buds in an unrooted R-tree.

To conclude this section, let us note that a simple way to generate the core of R-trees is to use a semi-developed representation of rooted R-trees, namely by only using the vertices of Fig. 4 (second line of Eq. (2.5)) and keeping S as a label, as illustrated in Fig. 6.

3.3. Enumeration of one-leg diagrams:

Let us now show that one-leg diagrams are in one-to-one correspondence with unrooted S-trees.

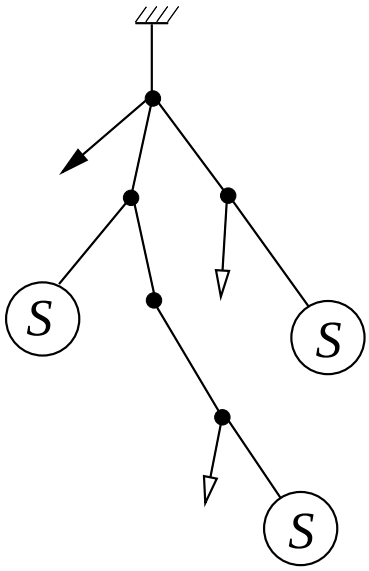

Fig. 6: The core of a typical rooted R-tree as obtained from the semi-developed representation using only the vertices of Fig. 4. Replacing the "leaves" marked with a label S by arbitrary rooted S-trees, we generate all rooted R-trees sharing the same rooted core.

Starting from an unrooted S-tree, we build a map by matching buds and leaves as in Ref. [10], by connecting iteratively each bud to the closest available leaf in *counterclockwise* direction as shown in Fig. 7, in such a way that the resulting graph is planar (i.e. with no intersection of edges). Such connected bud-leaf pairs are replaced by regular edges. As the total charge of 1 counts the number of leaves minus that of buds, the matching procedure leaves exactly one unmatched leaf which we replace by a distinguished univalent vertex. The net result is a one-leg diagram.

Conversely, starting from a one-leg diagram, we recover an unrooted S-tree by an inverse algorithm similar to that of Ref. [10]. Starting from the distinguished endpoint, we successively visit all edges adjacent to the external face in *counterclockwise* direction as shown in Fig. 8. At each step, the edge is cut iff the cutting does not disconnect the diagram. In the cutting procedure, the first half of the edge is replaced by a bud and the second half by a leaf. After one turn, the external face has been merged with all its adjacent faces. We then iterate the procedure until all faces have been merged. Replacing the distinguished endpoint by a leaf, the resulting connected diagram is an unrooted blossom tree with buds, leaves and regular vertices, and with total charge 1.

Let us now show that this tree actually is an S-tree by considering one of its inner edges (connecting regular vertices), which we denote by e (see Fig. 9). This edge separates the

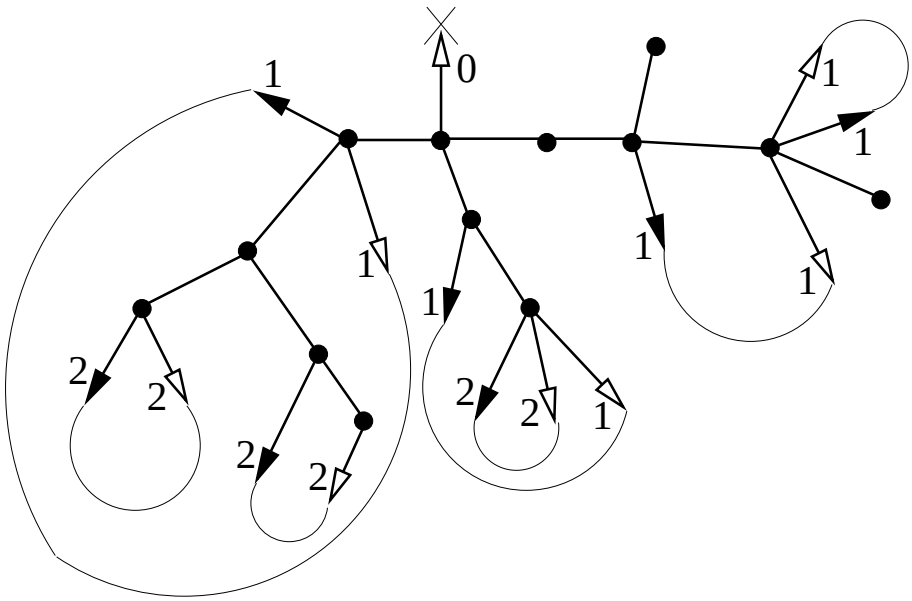

Fig. 7: A sample unrooted S-tree is closed into a one-leg diagram in a unique way, by iteratively matching each bud to the closest available leaf in counterclockwise direction. The resulting edges are indicated in thin solid lines, and form a system of non-intersecting arches around to the tree. We have also indicated for each bud and leaf the corresponding depth, namely that of the arch in the arch system, starting with depth 1 for arches adjacent to the external face. The unmatched vertex receives the depth 0 and serves as the distinguished endpoint of the one-leg diagram.

tree into two pieces, say T_1 and T_2, which contain all the vertices of the original diagram. We choose for T_1 the piece containing the distinguished endpoint. In the cutting procedure, e is not visited until all the other edges of the original diagram connecting a vertex of T_1 to one of T_2 have been visited once and cut into a bud-leaf pair. More precisely, these edges are replaced by a bud in T_1 and a leaf in T_2 when passing from T_1 to T_2 and *vice versa*. As the passings from T_1 to T_2 and from T_2 to T_1 alternate, these buds and leaves contribute by a net charge of 0 in both T_1 and T_2 if the number of passings is even, while they contribute by a net charge of -1 in T_1 and $+1$ in T_2 if the number is odd. Adding the charge $+1$ of the distinguished vertex changed into a leaf and noting that all other edges not connecting T_1 to T_2 have neutral contributions, we end up with two pieces of respective charges 0 and 1, the characterization of unrooted S-trees.

To further establish the bijection, it remains to prove that the two algorithms described above are inverse of each other. This is best seen by introducing the notion of *depth* of buds and leaves within an unrooted S-tree. Starting from a one-leg diagram and applying the above cutting algorithm, we may associate to each cut edge a natural "depth" $d = 1, 2, 3, ...$

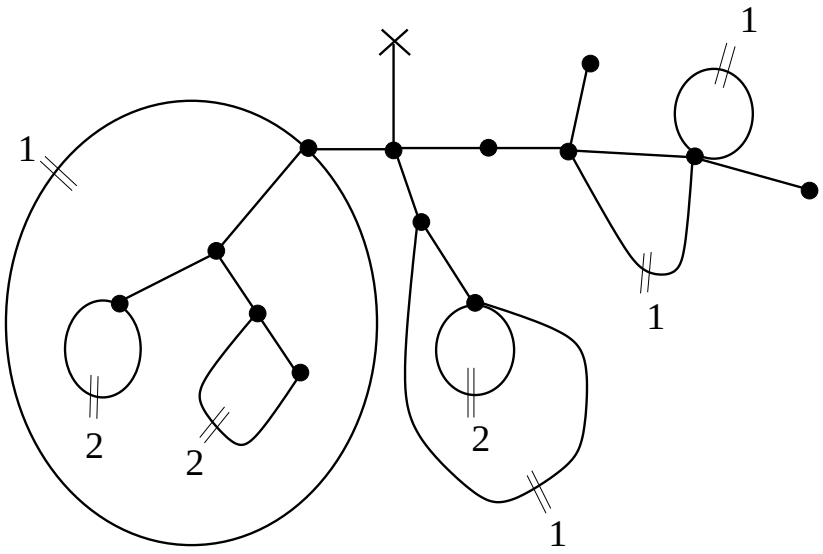

Fig. 8: A sample one-leg diagram is cut into an unrooted S-tree by visiting edges in counterclockwise direction around the diagram and iteratively cutting those which do not disconnect the remaining diagram, until a tree is obtained. The cut edges are indicated by a double-line, they are to be replaced by a bud, followed by a leaf. We have also indicated the depth of the corresponding cut edges, which will translate into the depths of buds and leaves of the S-tree. These depths correspond to the number of visits to the distinguished endpoint before the edge is cut.

by the number of visits to the distinguished vertex before this edge is cut. The same depth is attached to the corresponding bud and leaf, and finally the extra leaf replacing the distinguished vertex is given the depth 0. We have indicated the depths of buds and leaves in Figs. 7 and 8 for illustration. Remarkably, the depth is a notion intrinsic to the resulting unrooted S-tree. Indeed, in the bud-leaf matching procedure of an unrooted S-tree, the created edges form a system of arches around the tree and the depth of the buds and leaves is nothing but that of the corresponding arches, starting with depth 1 for external arches, and moreover associating the depth 0 to the unmatched leaf. This system of arches may also be constructed now as leaf-bud pairs of *decreasing* depth as follows. Starting from the depth 0 leaf we proceed *clockwise* around the tree and connect the first encountered leaf-bud pair of maximal depth, say k, and continue to connect leaves and buds of depth $k - \ell + 1$ after ℓ visits to the depth 0 leaf. This alternative closing procedure is the exact inverse of the cutting algorithm for one-leg diagrams.

As a direct consequence of the above bijection, the enumeration of one-leg diagrams is equivalent to that of unrooted S-trees. The latter is very simply performed by noting that there is one more leaf than bud in such a tree. The corresponding generating function

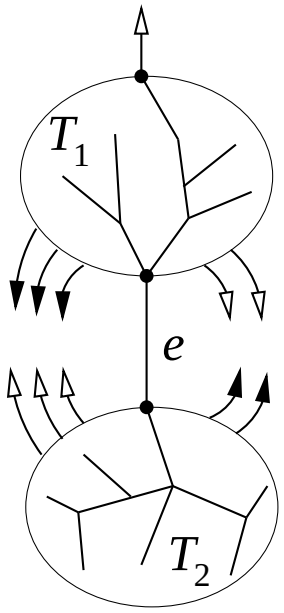

Fig. 9: The tree obtained by cutting a one-leg diagram is an unrooted S-tree. Any of its inner edges, e, separates the tree into two pieces T_1 and T_2, say with the distinguished endpoint in T_1. We have represented the cut bud-leaf pairs formerly connecting T_1 to T_2. The cutting procedure has successively cut these pairs in counterclockwise order around the edge e. In our example, there is one more bud-leaf pair on the left than on the right of e (odd number of passings). We could also have the same number of bud-leaf pairs on both sides (even number of passings). Collecting the total charge in T_1 and T_2 we see that in the case of the figure T_1 has charge 0 while T_2 has charge 1. In the case of an even number of passings, T_1 would have charge 1 and T_2 charge 0. This is the charge characterization of an unrooted S-tree.

is therefore equal to the difference between that of unrooted S-trees with a marked leaf and that of unrooted S-trees with a marked bud. The generating function of unrooted S-trees with a marked leaf is nothing but S as each of these leaves may be taken as a root. On the other hand, the generating function for unrooted S-trees with a marked bud is computed by noting that these trees are in one-to-one correspondence with rooted trees of total charge 2 whose descendent subtrees are buds, S- or R-trees, as is easily seen by replacing the marked bud by a neutral root. The generating function for unrooted S-trees with a marked bud therefore reads $V'(Q)|_{z^{-2}}$, leading to $\Gamma_1 = S - V'(Q)|_{z^{-2}}$ as in (2.6). QED.

3.4. Enumeration of two-leg diagrams:

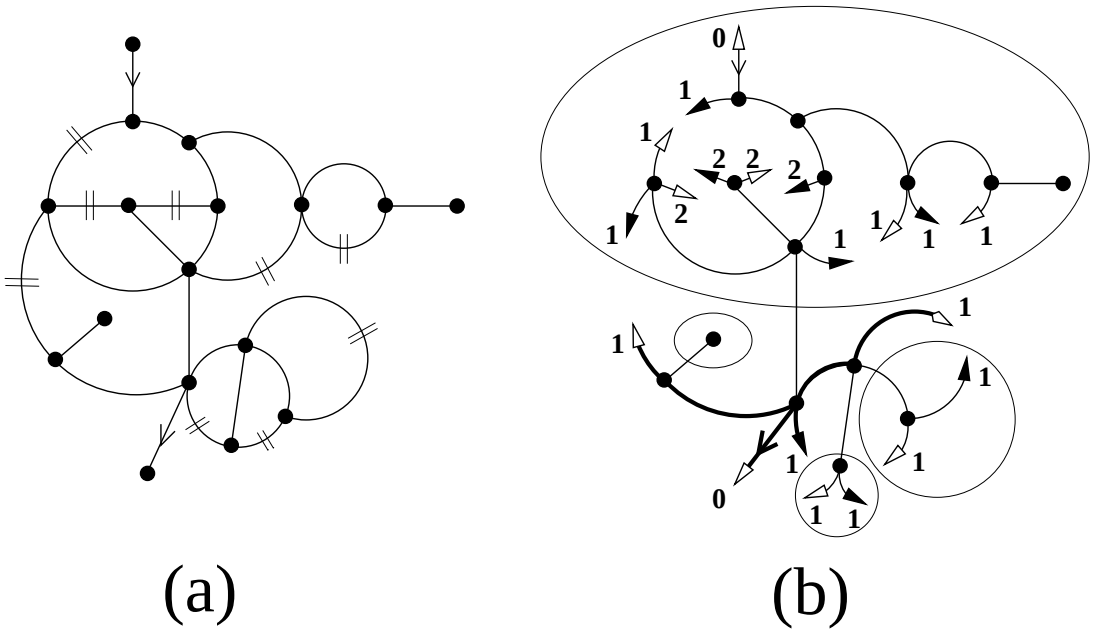

Fig. 10: A typical two-leg diagram (a) is cut into an unrooted R-tree (b) by first applying the cutting algorithm (cut edges are indicated by parallel thin lines in (a)) and then replacing the in- and out- coming endpoints by leaves. We have indicated the depths of the leaves and buds in the R-tree (b), as well as maximal S-subtrees (circled pieces) and the core to which they are attached (thickened edges). Note that the outgoing (depth 0) leaf is in the core, while the incoming one is not, as it lies in a maximal S-subtree. This gives an example of an unrooted R-tree in the set R_1, i.e. with exactly one depth 0 leaf in the core.

Let us now look for a similar equivalence in the case of two-leg diagrams. We will show that two-leg diagrams are in one-to-one correspondence with unrooted R-trees *with a marked leaf of depth* 0 *in the core*.

We apply the same cutting procedure as before to two-leg diagrams (see Fig. 10 (a)) starting from the *incoming* distinguished endpoint and finally replacing the two distinguished endpoints by leaves. The resulting tree (see Fig. 10 (b)) has total charge 2. Let us now show that: (i) it is an unrooted R-tree and (ii) the originally *outcoming* distinguished endpoint is a leaf belonging to the core. This is easily seen by noting that in the cutting procedure, the outcoming endpoint is treated as a regular univalent vertex. Therefore, viewing the original two-leg diagram as a one-leg diagram with an extra marked regular univalent vertex, we may apply the result of Section 3.3 showing that the resulting tree is an unrooted S-tree with this same marked regular univalent vertex. Cutting the edge leading to this vertex leaves us with two pieces, one rooted S-tree and one rooted R-tree.

Obviously, the S-tree is the piece made of the univalent vertex attached to a root. Therefore, the other piece is a rooted R-tree. This proves that picking the outcoming endpoint as a root leads to an R-tree showing both (i) and (ii) as the admissible roots are the leaves of the core.

Up to this point, we have never used the fact that the two endpoints of the diagram both lie in the external face. In fact, the above construction shows that R can be understood as the generating function $\Gamma_{1,1}$ of two-leg diagrams whose legs do not have to lie in the same face. This is also proved in appendix A in the matrix language. The requirement that the two endpoints belong to the external face implies a further restriction on the unrooted R-tree obtained through the cutting procedure, namely that the leaf replacing the outcoming endpoint has depth 0, as illustrated in Fig. 10 (b). As before, we indeed have an intrinsic notion of depth for unrooted R-trees, defined through the same bud-leaf counterclockwise matching algorithm. For unrooted R-trees, it now leads to two arch systems separated by two unmatched leaves. These two leaves are assigned a depth 0 while all the other buds or leaves are assigned the depth of the corresponding arch. For two-leg diagrams, the external legs naturally separate the edges to be cut into two independent arch system, showing that, when replaced by leaves, the incoming and outcoming endpoints both have depth 0 (see Fig. 10 (b)). Finally, the inverse of the above cutting procedure is easily identified as before with the suitable alternative matching algorithm connecting leaves and buds clockwise in decreasing depth order.

The enumeration of two-leg diagrams is finally reduced to that of unrooted R-trees with a marked leaf of depth 0 in the core. As a preliminary remark, note that there are exactly two leaves of depth 0 in an unrooted R-tree, which may or may not belong to the core. This suggests to classify the unrooted R-trees into three subsets R_0, R_1 and R_2 according to the number 0, 1 or 2 of depth 0 leaves in the core. For instance, the unrooted R-tree of Fig. 10 (b) belongs to R_1, as the incoming (depth 0) leaf lies in a maximal S-subtree (circled in the figure), while the outcoming one is in the core (represented by thickened edges in the figure). Denoting by R_0, R_1 and R_2 the corresponding generating functions, we have

$$\Gamma_2 = R_1 + 2R_2 = 2\tilde{R} - (R_1 + 2R_0) \tag{3.1}$$

where $\tilde{R} \equiv R_0 + R_1 + R_2$ is the generating function for unrooted R-trees.

$\tilde{R}$ can be computed as before by noting that there are exactly two more leaves than buds *in the core*. Hence $2\tilde{R}$ is the difference between the generating function for unrooted

R-trees with a marked leaf in the core, and that for unrooted R-trees with a marked bud in the core. The former is nothing but R according to Section 3.2. On the other hand, the generating function for unrooted R-trees with a marked bud in the core is computed by noting that these trees are in one-to-one correspondence with rooted trees of total charge 3 whose descendent subtrees are buds, S- or R-trees. This is seen again by replacing the marked bud by a neutral root and checking that all proper descendent subtrees not reduced to a bud have charge 0 or 1. Indeed such a descendent subtree either is itself a descendent of an S-subtree, hence has charge 0 or 1, or originates from an edge of the core, hence has charge 1. The generating function for unrooted R-trees with a marked bud in the core therefore reads $V'(Q)|_{z^{-3}}$, leading to $2\tilde{R} = R - V'(Q)|_{z^{-3}}$. Remark that the accidental two-fold symmetry of unrooted R-trees is properly accounted for in $\tilde{R}$ in which symmetric contributions (which contribute only once to R and $V'(Q)|_{z^{-3}}$) receive a weight 1/2.

The remaining term in Eq. (3.1) can be computed with the result $(R_1 + 2R_0) = (V'(Q)|_{z^{-2}})^2$. The proof is slightly tedious and is detailed in appendix B.

This finally allows to express Eq. (3.1) in the form of Eq. (2.6). QED.

4. Discussion

4.1. Cubic maps

The first non-trivial case of planar maps is that of *cubic* maps, namely maps whose regular vertices are all trivalent (closed planar cubic maps are dual to triangulations of the sphere). These correspond in our notations to taking $g_k = g\delta_{k,3}$, in which case $V'(Q) = gQ^2$, and the fundamental relations (2.5) read

$$\begin{aligned} S &= gt(S^2 + 2R) \\ R &= t + 2gtRS \end{aligned} \tag{4.1}$$

while the one- and two-leg diagram generating functions read

$$\begin{aligned} \Gamma_1 &= S - gR^2 \\ \Gamma_2 &= R - g^2R^4 \end{aligned} \tag{4.2}$$

Note that S- and R-trees are now binary trees, as they originate from cubic maps. In this particular case, we also have the following additional relation

$$\Gamma_1 = gt(\Gamma_2 + \Gamma_1^2) \tag{4.3}$$

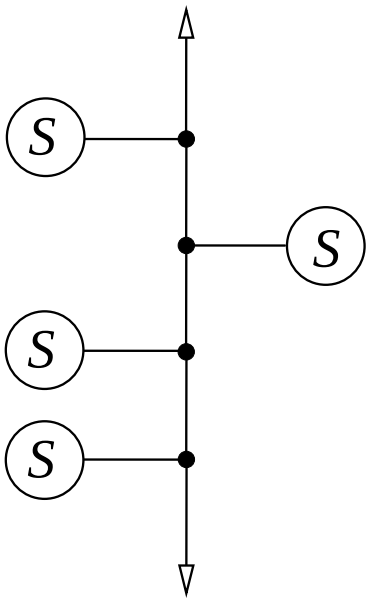

Fig. 11: In the cubic map case, the core of a typical unrooted R-tree is a chain with a leaf at each end and attached maximal S-subtrees on either side.

obtained by cutting out from any one-leg diagram the leg and the trivalent vertex connected to it: the remaining part is made either of a connected two-leg diagram (term in Γ_2) or of two disconnected one-leg diagrams (contributing to a term in Γ_1^2). Alternatively, the relation (4.2) is also easily proved by use of Eqs. (4.1) and (4.2).

Another drastic simplification is that the core of any unrooted R-tree is a simple chain joining two leaves, with no buds and with attached maximal S-trees (see Fig. 11). The absence of buds is a consequence of $V'(Q)|_{z^{-3}} = 0$ in this case, leading moreover to $2\tilde{R} = R$, as there are two admissible leaves that can serve as roots.

The actual numbers of S- and R-trees as well as one- and two-leg diagrams with fixed number of edges are obtained by first eliminating R from Eq. (4.1), and then applying the Lagrange inversion formula. Introducing the rescaled functions and variables $\sigma = gtS$, $\rho = (gt)^2 R$, $\theta = g^2 t^3$, we get

$$\begin{aligned} 2\theta &= \sigma(1-\sigma)(1-2\sigma) \\ \rho &= \frac{\sigma(1-\sigma)}{2} \end{aligned} \tag{4.4}$$

Denoting by $\varphi(\sigma) = \sigma(1-\sigma)(1-2\sigma)$, we may now express the series expansion in θ of any function $h(\sigma)$ (with $h(0) = 0$) through the Lagrange inversion formula, a direct

consequence of the Cauchy formula:

$$\begin{aligned} h(\sigma) &= \oint \frac{ds}{2i\pi} \frac{h(s)\varphi'(s)}{\varphi(s)-\varphi(\sigma)} \\ &= \sum_{n=1}^{\infty} \frac{(2\theta)^n}{n} \oint \frac{ds}{2i\pi} \frac{h'(s)}{\varphi(s)^n} \end{aligned} \tag{4.5}$$

where we have used the first line of (4.4) and integrated by parts. Upon picking respectively $h(x) = x$ and $h(x) = x(1-x)/2$, we get the series coefficients σ_n and ρ_n for $S = (gt)^{-1} \sum_{n=1}^{\infty} \sigma_n \theta^n$ and $R = (gt)^{-2} \sum_{n=1}^{\infty} \rho_n \theta^n$ as contour integrals, easily calculated as $\sigma_1 = 2$, $\rho_1 = 1$ and for $n \geq 2$:

$$\begin{aligned} \sigma_n &= \frac{2^n}{n} \oint \frac{ds}{2i\pi s^n} \frac{1}{(1-s)^n(1-2s)^n} \\ &= \frac{2^n}{n} \sum_{k=0}^{n} 2^k \binom{2n-k-2}{n-1} \binom{n+k-1}{n-1} \\ &= \frac{2^{2n-1}}{n!}(n+1)(n+3)...(3n-5)(3n-3) \\ \rho_n &= \frac{2^{n-1}}{n} \oint \frac{ds}{2i\pi s^n} \frac{1}{(1-s)^n(1-2s)^{n-1}} \\ &= \frac{2^{n-1}}{n} \sum_{k=0}^{n} 2^k \binom{2n-k-2}{n-1} \binom{n+k-2}{n-2} \\ &= \frac{2^{2n-2}}{n!} n(n+2)(n+4)...(3n-6)(3n-4) \end{aligned} \tag{4.6}$$

for the numbers σ_n, ρ_n of rooted S- and R-trees with n leaves.

Similarly, we get expressions for the numbers of one- (resp. two-) leg diagrams with $3n-1$ (resp. $3n-2$ edges), denoted by $\gamma_n^{(1)}$ (resp. $\gamma_n^{(2)}$) by expressing the relevant generating functions in terms of σ only, with the result $\gamma_1^{(1)} = 1$, $\gamma_1^{(2)} = 1$ and for $n \geq 2$:

$$\begin{aligned} \gamma_n^{(1)} &= \frac{2^{2n-1}}{(n+1)!}(n+1)(n+3)...(3n-5)(3n-3) \\ \gamma_n^{(2)} &= \frac{3}{n+2} \frac{2^{2n-2}}{n!} n(n+2)(n+4)...(3n-6)(3n-4) \end{aligned} \tag{4.7}$$

As a direct consequence of the S-tree conjugacy, we have $\gamma_n^{(1)} = \sigma_n/(n+1)$, as a corresponding unrooted S-tree has exactly $n+1$ leaves which all may serve as a root in the conjugacy class. We note a slightly less trivial relation between the numbers of two-leg diagrams and R-trees: $\gamma_n^{(2)} = 3\rho_n/(n+2)$ which still awaits a good combinatorial interpretation.

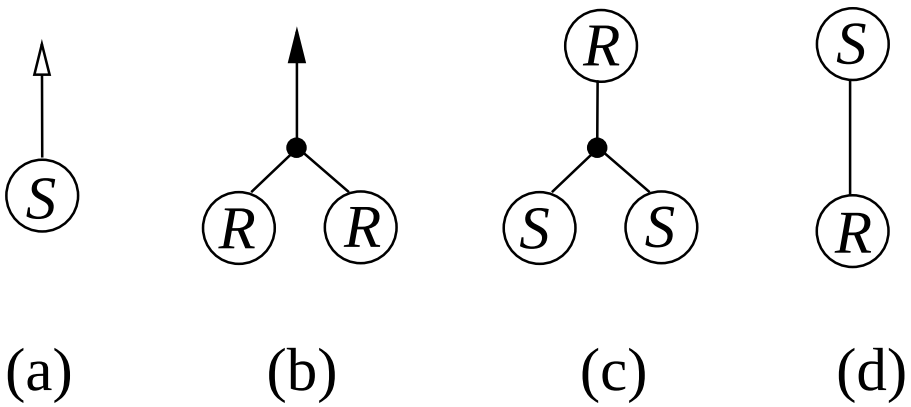

Fig. 12: The local environment in an unrooted S-tree in the cubic case around (a) a leaf, (b) a bud, (c) a vertex with no bud, and (d) an edge not leading to a bud.

Finally, we get the number e_n of rooted cubic maps with $3n$ edges by substituting Eq. (4.3) into Eq. (2.1), leading to $E = \Gamma_1/(gt^2) - 1$, and therefore

$$e_n = \gamma_{n+1}^{(1)} = \frac{2^{2n+1}}{(n+2)!}(n+2)(n+4)(n+6)...(3n-2)(3n) \tag{4.8}$$

for all $n \geq 1$.

Introducing the rescaled one-leg diagram generating function $G_1 = gt\Gamma_1$, we easily get the following differential equations

$$\begin{aligned} \left(\theta\frac{d}{d\theta} + 1\right) G_1 &= \sigma \\ \theta\frac{d}{d\theta} G_1 &= \frac{\rho^2}{\theta} \\ \left(\theta\frac{d}{d\theta} - 1\right) G_1 &= \frac{\rho\sigma^2}{\theta} \\ \left(3\theta\frac{d}{d\theta} - 1\right) G_1 &= \frac{\rho\sigma}{\theta} \end{aligned} \tag{4.9}$$

obtained by marking in an unrooted S-tree respectively a leaf, a bud, a trivalent vertex with no bud and an edge, in respective numbers $n+1$, n, $n-1$, $3n-1$. The combinatorial origin of these relations is depicted in Fig. 12.

4.2. Eulerian maps

The case of Eulerian maps, namely of diagrams with only regular vertices of *even valences* was solved by Tutte [3], and takes a much simpler form than the general case.

Eulerian maps may be recovered here by demanding that V be an even function, namely that all $g_{2k-1} = 0$, $k = 1, 2, ...$ The matrix model solution (see appendix A) shows in that case that $S = 0$ as a consequence of the symmetry $x \to -x$ of the planar eigenvalue density. From the present combinatorial point of view, it is easy to see that the recursion relations of Figs. 3 and 4 lead to infinite rooted trees unless we decide that there are no rooted S-trees at all. In other words, our finiteness requirement forces us to take the trivial generating function $S = 0$.

With this simplification, we are left with only rooted R-trees, which become the fundamental combinatorial objects, now characterized by the property that (i) their total charge is 1 and (ii) all their descendent subtrees not reduced to a bud have charge 1 as well (thus are themselves R-trees). These trees are those which have been considered in Ref. [10] in the original connection between Eulerian maps and conjugated trees. Moreover, in the absence of S-trees, it is easy to see that the core of an unrooted R-tree is actually the whole tree itself, with all the leaves as admissible roots. The notion of conjugacy therefore becomes much simpler and coincides with that used in Ref. [10].

5. Conclusion

In this paper, we have elucidated the combinatorial structure of the one-matrix model solution to the problem of enumerating planar maps with prescribed vertex degrees. Our construction generalizes that of Ref. [10] for Eulerian maps using two types of trees instead of one and a refined notion of conjugacy of trees. The need for these two types of trees is inherent to the absence of (twofold) symmetry in arbitrary planar graphs as opposed to Eulerian ones (face bicolorability) which can be traced back to the absence of $\mathbb{Z}_2$ symmetry in the matrix model.

Here we have considered arbitrary graphs with no restrictions on reducibility. *Irreducible maps* were enumerated in some particular cases by Tutte [1] [2] [4] and a connection with conjugated trees was obtained recently in Ref. [11]. In the matrix integral language, the construction of (p-particle) irreducible diagrams can be performed as already shown in [6] through appropriate renormalizations. It does not involve the introduction of new fundamental objects and we therefore believe that the corresponding enumeration can be understood also in terms of S- and R- trees.

Finally, we have many other solvable matrix models at hand and we may expect that, for some of them, the underlying combinatorics can be understood directly in terms of

appropriate conjugated trees. This is already the case for particular two-matrix models, describing the enumeration of bipartite regular graphs, recently reformulated in terms of conjugated trees [12-15]. The hope is that it may also apply for instance to the case of interacting two matrix models such as that describing the two-dimensional Ising model [16] or hard particle model [17] on random lattices. This also suggests to look for a more general picture relating the tree structure to the (Toda-like) integrable structure of matrix models.

Appendix A. Planar maps from the one matrix model

In this appendix, we recall the derivation of the planar limit of the integral (2.2). For the sake of technical simplicity, we must take for the potential $V(x)$ a truncated polynomial form namely

$$V(x) = \sum_{k=1}^{I} g_k \frac{x^k}{k} \tag{A.1}$$

The result is then trivially extended so as to involve arbitrarily many g_k's.

The planar limit of the integral (2.2) is evaluated in a succession of standard steps as follows (see e.g. Refs. [7] and [8] for details). The first step consists in reducing the integral (2.2) to one over the eigenvalues of M. This is readily done by changing variables $M \to (m, U)$, where $M = UmU^\dagger$, and m is a real diagonal matrix, while $U \in U(N)/U(1)^N$ is a unitary matrix defined up to the right multiplication by an arbitrary diagonal matrix with entries of the form $e^{i\phi_j}$ with real phases ϕ_j, $j = 1, 2, ..., N$. The Jacobian of this change of variables reads $J = \Delta(m)^2$, where $\Delta(m) = \det(m_i^{j-1})|_{1 \le i,j \le N}$ is the Vandermonde determinant of m. As the integrand of (2.2) only depends on m, the angular variables U may be integrated out, with the result

$$Z_N(t, \{g_k\}) = \int dm \Delta(m)^2 e^{-N \mathrm{Tr}\left(\frac{m^2}{2t} - V(m)\right)} \tag{A.2}$$

up to an overall unimportant multiplicative constant (the volume of the angular variables' locus).

The second step consists in evaluating the large N limit of (A.2) by putting this integral into a more familiar form, and evaluating it via a saddle-point method. Indeed, introducing the functional

$$S(m) = \frac{1}{N} \sum_{i=1}^{N} \left(\frac{m_i^2}{2t} - V(m_i) \right) - \frac{1}{N^2} \sum_{1 \le i \ne j \le N} \mathrm{Log}\, |m_i - m_j| \tag{A.3}$$

the integral (A.2) takes the form $Z_N = \int dm e^{-N^2 S(m)}$. In the limit of large N, this integral is dominated by the solution m to the saddle-point equations $\partial S/\partial m_i = 0$, namely

$$\frac{m_i}{t} - V'(m_i) = \frac{1}{N} \sum_{\substack{j=1 \\ j \neq i}}^{N} \frac{1}{m_i - m_j} \tag{A.4}$$

In particular, we get the planar (genus zero) free energy of the model as the limit

$$f(t, \{g_k\}) \equiv \lim_{N \to \infty} \frac{1}{N^2} \mathrm{Log}\, Z_N(t, \{g_k\}) = -S(m) \tag{A.5}$$

evaluated at the solution m to (A.4). To further compute this solution, let us introduce the resolvent $\omega_N(\zeta)$

$$\omega_N(\zeta) = \frac{1}{N} \sum_{i=1}^{N} \frac{1}{\zeta - m_i} \tag{A.6}$$

evaluated on the solution m to (A.4). This function is related to the eigenvalue density $\rho_N(\zeta)$ defined as

$$\rho_N(\zeta) = \frac{1}{N} \sum_{i=1}^{N} \delta(\zeta - m_i) \tag{A.7}$$

also evaluated on the solution m to (A.4). More precisely we have $\rho_N(\zeta) = (\omega(\zeta + i0) - \omega(\zeta - i0))/(2i\pi)$, so the density of eigenvalues is concentrated on the (real) singularities of ω_N. By the definition (A.6), it is easy to see that $\omega_N(\zeta) \sim 1/\zeta$ when ζ is large, expressing the normalization of the density $\int_{\mathbb{R}} dx \rho_N(x) = 1$. Let us now multiply both sides of (A.4) by $1/(\zeta - m_i)$ and sum over $i = 1, 2, ..., N$. We find the following simple quadratic differential equation for $\omega_N(\zeta)$

$$\frac{1}{N} \frac{d\omega_N(\zeta)}{d\zeta} = \omega_N(\zeta)^2 - \left(\frac{\zeta}{t} - V'(\zeta) \right) \omega_N(\zeta) + P_N(\zeta) \tag{A.8}$$

where $P_N(\zeta)$ is defined by

$$P_N(\zeta) = \frac{1}{t} - \frac{1}{N} \sum_{i=1}^{N} \frac{V'(m_i) - V'(\zeta)}{m_i - \zeta} \tag{A.9}$$

Note that, as V' is a polynomial of degree $I - 1$, P_N is itself a polynomial of degree $I - 2$. In the large N limit, the left hand side of (A.8) is negligible, and we may therefore obtain the large N resolvent $\omega(\zeta) \equiv \lim_{N \to \infty} \omega_N(\zeta)$ as the solution of a quadratic equation, in the form

$$\omega(\zeta) = \frac{1}{2} \left(\frac{\zeta}{t} - V'(\zeta) \pm \sqrt{(\frac{\zeta}{t} - V'(\zeta))^2 - 4P(\zeta)} \right) \tag{A.10}$$

where P denotes the large N limit of P_N (it is also a polynomial of degree $I-2$), and the sign $\pm$ is selected by requiring that the large ζ asymptotics of $\omega(\zeta)$ read $\omega(\zeta) \sim 1/\zeta$.

In a third step, the planar resolvent $\omega(\zeta)$ is further completely fixed by making the standard "one-cut" hypothesis, namely that $\omega(\zeta)$ only has a square root singularity of the form $\sqrt{(\zeta-a)(\zeta-b)}$ where a and b are real, with say $a<b$. This expresses the fact that the planar eigenvalue density $\rho(\zeta) \equiv \lim_{N\to\infty} \rho_N(\zeta)$ is assumed to have a compact support made of *a single real interval* $[a,b]$. Picking say g_I to be positive, the sign in (A.10) is fixed to be $+$, and the resolvent takes the form

$$\omega(\zeta) = \frac{1}{2}\left(\frac{\zeta}{t} - V'(\zeta) + G(\zeta)\sqrt{(\zeta-a)(\zeta-b)}\right) \tag{A.11}$$

where $G(\zeta)$ is a polynomial of degree $I-2$. Writing that $\omega(\zeta) \sim 1/\zeta$ at large ζ now determines all coefficients of G and both a and b. More precisely, we have

$$G(\zeta) = \left[\frac{V'(\zeta) - \frac{\zeta}{t}}{\sqrt{(\zeta-a)(\zeta-b)}}\right]_+ \tag{A.12}$$

where we must expand the bracket as a power series of ζ at ∞, and the subscript $+$ indicates that we must retain only the polynomial part of this Laurent series. Denoting moreover by $H(\zeta) = (V'(\zeta) - \frac{\zeta}{t})/\sqrt{(\zeta-a)(\zeta-b)}$ the Laurent series in the bracket, we may express directly

$$\omega(\zeta) = -\frac{1}{2}[H(\zeta)]_- \sqrt{(\zeta-a)(\zeta-b)} \tag{A.13}$$

where the subscript $-$ indicates that we only retain negative powers of ζ in the Laurent series. Using the Cauchy formula around the infinity in the complex plane, we may express the coefficients of $[H(\zeta)]_- = \sum_{m\geq 1} \zeta^{-m} H(\zeta)|_{\zeta^{-m}}$ as

$$H(\zeta)|_{\zeta^{-m}} = \frac{1}{2i\pi}\oint w^{m-1} dw \frac{V'(w) - \frac{w}{t}}{\sqrt{(w-a)(w-b)}} \tag{A.14}$$

This integral may be drastically simplified if we change variables to z:

$$w = Q(z) \equiv z + S + \frac{R}{z} \tag{A.15}$$

and pick R and S so that the square root disappears. Indeed,

$$(w-a)(w-b) = z^2 + (2S-a-b)(z+\frac{R}{z}) + (S-a)(S-b) + 2R + \frac{R^2}{z^2} \tag{A.16}$$

is a perfect square iff

$$S = \frac{a+b}{2}$$
$$R = \left(\frac{b-a}{4}\right)^2 \tag{A.17}$$

in which case $\sqrt{(w-a)(w-b)} = z - R/z$ around the infinity. The change of variables $w \to z$ then leads to

$$H(\zeta)|_{\zeta^{-m}} = \frac{1}{2i\pi}\oint \frac{dz}{z}\left(V'(Q(z)) - \frac{Q(z)}{t}\right)Q(z)^{m-1} \tag{A.18}$$

For the first few values of $m = 1, 2, 3, 4$, this gives

$$\begin{aligned}
H(\zeta)|_{\zeta^{-1}} &= V'(Q)|_{z^0} - \frac{S}{t} \\
H(\zeta)|_{\zeta^{-2}} &= 2\big(V'(Q)|_{z^{-1}} - \frac{R}{t}\big) + SH(\zeta)|_{\zeta^{-1}} \\
H(\zeta)|_{\zeta^{-3}} &= 2V'(Q)|_{z^{-2}} + 2SH(\zeta)|_{\zeta^{-2}} + (2R - S^2)H(\zeta)|_{\zeta^{-1}} \\
H(\zeta)|_{\zeta^{-4}} &= 2V'(Q)|_{z^{-3}} + 3SH(\zeta)|_{\zeta^{-3}} + 3(R - S^2)H(\zeta)|_{\zeta^{-2}} + (S^3 - 3RS)H(\zeta)|_{\zeta^{-1}}
\end{aligned} \tag{A.19}$$

In the second, third and fourth lines of (A.19), we have used the symmetry $z \leftrightarrow R/z$ of the change of variables to express that $f(Q)|_{z^{-m}} = R^m f(Q)|_{z^m}$ for any Laurent series f, and all $m \geq 0$, in order to reexpress the result in terms mostly of $V'(Q)$. We now simply have to substitute the above expressions for the coefficients of H into the formula (A.13) for $\omega(\zeta)$, and impose that $\omega(\zeta) = 1/\zeta + O(1/\zeta^2)$ at infinity. This gives respectively for the order ζ^0 and ζ^{-1} terms the two equations

$$\begin{aligned}
\frac{S}{t} - V'(Q)|_{z^0} &= 0 \\
\frac{R}{t} - V'(Q)|_{z^{-1}} &= 1
\end{aligned} \tag{A.20}$$

which are nothing but (2.5).

The planar resolvent $\omega(\zeta)$ may also be used as the generating function for the quantities $\theta_k = \lim_{N\to\infty} \frac{1}{N}\langle \mathrm{Tr}(M^k)\rangle$ that enumerate the (possibly disconnected) planar maps with one special k-valent vertex and arbitrary regular m-valent ones weighted by g_m, $m = 1, 2, 3, ...$ and with a weight t per edge. Indeed, the definition of $\omega(\zeta)$ entails that

$$\omega(\zeta) = \sum_{k=0}^{\infty} \zeta^{-k-1} \lim_{N\to\infty} \frac{1}{N}\mathrm{Tr}(m^k) = \sum_{k=0}^{\infty} \zeta^{-k-1}\theta_k \tag{A.21}$$

where m stands for the solution to the saddle-point equations (A.4). In particular, let us use the direct expression (A.13) to compute the coefficients θ_1 and θ_2 corresponding to one and two-leg diagrams respectively. Substituting (A.19) into (A.13), we get

$$\begin{aligned} \theta_1 &= S - V'(Q)|_{z^{-2}} \\ \theta_2 &= R + S^2 - V'(Q)|_{z^{-3}} - 2SV'(Q)|_{z^{-2}} \end{aligned} \tag{A.22}$$

Finally, we note that the one-leg diagrams counted by θ_1 are always connected hence $\theta_1 = \Gamma_1$, while the two-leg ones may be disconnected, and we must write $\Gamma_2 = \theta_2 - \theta_1^2$. This finally leads to Eqs. (2.6).

A first remark is in order. The quantity R may be directly expressed as a connected matrix average, namely

$$R = \theta_{1,1} - \theta_1^2 \tag{A.23}$$

where

$$\theta_{1,1} = \lim_{N\to\infty} \frac{1}{N^2} \langle \mathrm{Tr}(M)\, \mathrm{Tr}(M) \rangle \tag{A.24}$$

where the average is computed by attaching two external legs to connected planar maps and those two legs *do not have to lie in the same face* (as they do in Γ_2). To prove this, the simplest way is to use the linear term in the potential to generate insertions of $\mathrm{Tr}(M)$ by differentiating with respect to g_1. For instance, the connected average $\Gamma_{1,1} \equiv \theta_{1,1} - \theta_1^2$ is easily obtained by differentiating θ_1 with respect to g_1:

$$\begin{aligned} \Gamma_{1,1} &= \frac{\partial \theta_1}{\partial g_1} \\ &= \frac{\partial S}{\partial g_1} - \frac{\partial V'(Q)|_{z^{-2}}}{\partial g_1} \\ &= (1 - V''(Q)|_{z^{-2}}) \frac{\partial S}{\partial g_1} - V''(Q)|_{z^{-1}} \frac{\partial R}{\partial g_1} \end{aligned} \tag{A.25}$$

Let us now use the second equation of (A.20) to express the 1 in the first factor as $1 = R/t - V'(Q)|_{z^{-1}}$, and upon differentiating the first line of (A.20) with respect to g_1 and multiplying by R, we may eliminate $(R/t)\partial S/\partial g_1 - V''(Q)|_{z^{-1}} \partial R/\partial g_1 = R + RV''(Q)|_{z^0} \partial S/\partial g_1$, to get

$$\Gamma_{1,1} = R + (RV''(Q)|_{z^0} - V'(Q)|_{z^{-1}} - V''(Q)|_{z^{-2}}) \frac{\partial S}{\partial g_1} \tag{A.26}$$

Finally, it is easy to see that the prefactor of $\partial S/\partial g_1$ vanishes, as it is nothing but the residue of a total derivative: $-\frac{d}{dz}\big(zV'(Q)\big)|_{z^{-1}} = 0$. We finally get the desired result $\Gamma_{1,1} = R$.

A last remark is in order. When all $g_{2k-1} = 0$, $k = 1, 2, 3, ...$, the partition function (2.2) counts possibly disconnected Eulerian maps, namely with only regular vertices of even valence. In our present formulation, we see that the complete potential $\frac{x^2}{2t} - V(x)$ is an even function of x, which simplifies the results considerably. Indeed, we may immediately infer that the planar density of eigenvalues is also even, so that $a+b = 0$, henceforth $S = 0$.

Appendix B. Proof of the relation $R_1 + 2R_0 = (V'(Q)|_{z^{-2}})^2$

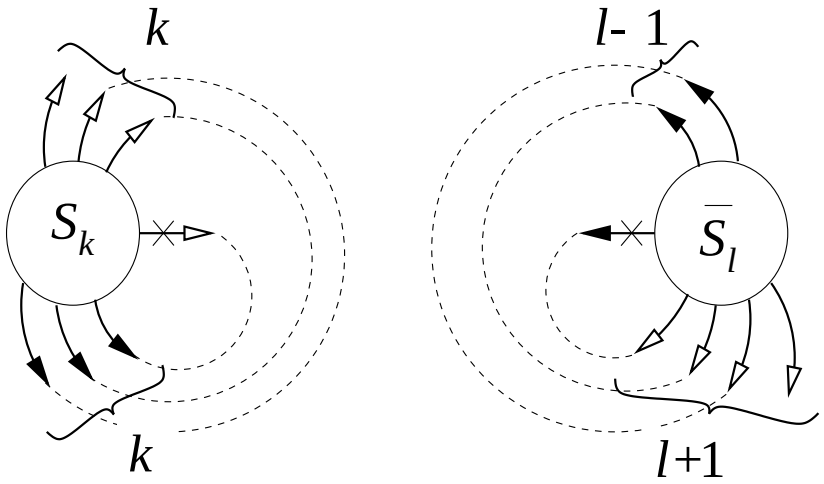

Fig. 13: A schematic representation of an S_k-tree (on the left) and of an $\bar{S}_l$-tree (on the right). We represent only the buds and leaves which play a role in the evaluation of the depth of the marked (by a cross) leaf or bud. We also indicate the closing arches in dashed lines.

Let us introduce refined definitions of S-trees as follows. We define an S_k- (resp. an $\bar{S}_l$-) tree as an unrooted S-tree with a marked leaf (resp. a marked bud) of depth k (resp. l). An illustration of these definitions is given in Fig. 13. We denote by S_k (resp. $\bar{S}_l$) the corresponding generating functions. As the number of leaves and buds of given depth $k \geq 1$ are the same in any unrooted S-tree, we have $S_k = \bar{S}_k$ for all $k \geq 1$. For $k = 0$ we have $\bar{S}_0 = 0$ while $S_0 = \Gamma_1$ as there is a unique depth 0 leaf in any unrooted S-tree. Moreover we have $S = \sum_{k \geq 0} S_k$ as the choice of root for an S-tree is that of a leaf of arbitrary depth. Using the first line of (2.6) (for which we have already given a combinatorial proof in Section 3.3), we may express

$$V'(Q)|_{z^{-2}} = S - \Gamma_1 = \sum_{k \geq 1} S_k = \sum_{k \geq 1} \bar{S}_k \tag{B.1}$$

and therefore

$$(V'(Q)|_{z^{-2}})^2 = \sum_{k\geq 1} S_k \bar{S}_k + 2 \sum_{k>l\geq 1} S_k \bar{S}_l \tag{B.2}$$

Let us now identify the right hand side of this equation with $R_1 + 2R_0$.

The quantity $S_k \bar{S}_l$ counts all trees obtained by gluing into an edge the marked leaf of an S_k-tree with the marked bud of an $\bar{S}_l$-tree. The resulting tree is easily seen to be an unrooted R-tree (of total charge 2) with a particular marked edge. This edge separates the unrooted R-tree into a rooted S-subtree (the former S_k-tree with its marked leaf replaced by a root) and a part of charge 2 (obtained by removing the marked bud of the $\bar{S}_l$-tree). Let us show that the S-subtree is maximal hence the marked edge connects it to the core of the unrooted R-tree. Indeed, the maximal S-tree containing this S-subtree is connected to the core through a 0-2 edge. This edge separates the $\bar{S}_l$-tree into a piece of charge 2 and one of charge -1, which in an unrooted S-tree is possible only if the part of charge -1 is reduced to a bud. This identifies the above 0-2 edge with the marked one, and proves that the S-subtree is maximal. Note moreover that the core of the R-tree is actually obtained by gluing the cores of all the R-subtrees of the $\bar{S}_l$-tree originating from the vertex to which the marked bud is attached. The quantity $S_k \bar{S}_l$ counts unrooted R-trees with a singularized maximal S-subtree and particular depth restrictions.

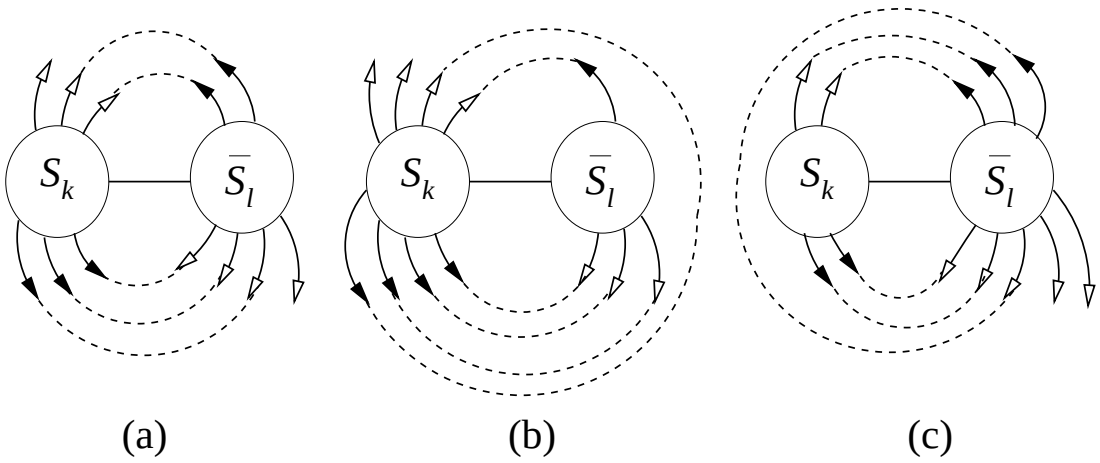

Fig. 14: A schematic view of the unrooted R-tree resulting from the connection of an S_k-tree with an $\bar{S}_l$-tree via their marked leaf and bud. The positions of the two unmatched leaves in the closing procedure depend on whether (a) $k = l$ (one on each side) (b) $k > l$ (both on the left) or (c) $k < l$ (both on the right).

Now it is easy to check that if $k = l$, the bud-leaf matching procedure leaves us with *one unmatched leaf on each side* (see Fig. 14). On the other hand, for $k \neq l$, the two unmatched leaves are on the same side, which is that of the singularized maximal S-subtree iff $k > l$. The right hand side of (B.2) therefore counts the number of unrooted R-trees with a singularized maximal S-subtree and with a marked depth 0 leaf on it. This also counts the unrooted R-trees twice if their two depth 0 leaves lie outside the core (i.e. in either the same or two distinct maximal S-subtrees), and once if exactly one depth 0 leaf lies outside the core (i.e. is in a maximal S-subtree). This is nothing but $2R_0 + R_1$. QED.

References

[1] W. Tutte, *A Census of planar triangulations* Canad. Jour. of Math. **14** (1962) 21-38.

[2] W. Tutte, *A Census of Hamiltonian polygons* Canad. Jour. of Math. **14** (1962) 402-417.

[3] W. Tutte, *A Census of slicings* Canad. Jour. of Math. **14** (1962) 708-722.

[4] W. Tutte, *A Census of Planar Maps*, Canad. Jour. of Math. **15** (1963) 249-271.

[5] G. 't Hooft, *A planar diagram theory for strong interactions*, Nucl. Phys. **B72** (1974) 461-473.

[6] E. Brézin, C. Itzykson, G. Parisi and J.-B. Zuber, *Planar Diagrams*, Comm. Math. Phys. **59** (1978) 35-51.

[7] P. Di Francesco, P. Ginsparg and J. Zinn–Justin, *2D Gravity and Random Matrices*, Physics Reports **254** (1995) 1-131.

[8] B. Eynard, *Random Matrices*, Saclay Lecture Notes (2000), available at *http://www-spht.cea.fr/lectures_notes.shtml*

[9] G. Schaeffer, *Conjugaison d'arbres et cartes combinatoires aléatoires* PhD Thesis, Université Bordeaux I (1998).

[10] G. Schaeffer, *Bijective census and random generation of Eulerian planar maps*, Electronic Journal of Combinatorics, vol. 4 (1997) R20.

[11] D. Poulhalon and G. Schaeffer, *A bijection for loopless triangulations of a polygon with interior points*, proceedings of the conference FPSAC'02, Melbourne (2002), available at *http://www.loria.fr/∼schaeffe/*

[12] M. Bousquet-Mélou and G. Schaeffer, *Enumeration of planar constellations*, Adv. in Applied Math., **24** (2000) 337-368.

[13] D. Poulhalon and G. Schaeffer, *A note on bipartite Eulerian planar maps*, preprint (2002), available at *http://www.loria.fr/∼schaeffe/*

[14] P. Di Francesco, B. Eynard and E. Guitter, *Coloring Random Triangulations*, Nucl. Phys. **B516 [FS]** (1998) 543-587.

[15] J. Bouttier, P. Di Francesco and E. Guitter, *Counting colored Random Triangulations*, Saclay preprint SPhT/02-075, cond-mat/0206452, to appear in Nucl. Phys. B.

[16] see for instance D. Boulatov and V. Kazakov, *The Ising model on a random planar lattice: the structure of the phase transition and the exact critical exponents*, Phys. Lett. **B186** (1987) 379-384.

[17] J. Bouttier, P. Di Francesco and E. Guitter, *Critical and tricritical hard objects on bicolourable random lattices: exact solutions* J. Phys. A: Math. Gen. **35** (2002) 3821-3854.